Optical properties of ZnO:TM (TM = Cr, Mn and Co) layers obtained by pulsed laser deposition technique

[1] Potera P., [1, 2] Virt I., [1] Cieniek B. and [1] Wisz G.

[1] Faculty of Mathematics and Natural Sciences University of Rzeszow, Aleja Tadeusza Rejtana 16C, 35-310, Rzeszów Rzeszow, Poland
[2] Drohobych State Pedagogical University, Ivan Franko Str., 24, Drohobych, 82100, Ukraine

Received: 23.07.2019

Abstract. We study the optical properties of zinc-chromium (ZnCrO), zinc-manganese (ZnMnO) and zinc-cobalt (ZnCoO) oxide layers grown on sapphire substrates, using a pulsed laser deposition technique. The influence of target composition and post-growth annealing on the optical transmission of the films and their bandgap energy are analyzed.

Keywords: zinc oxides, pulsed laser deposition, optical transmission spectra

UDC: 535.343.2

1. Introduction

Zinc oxide belonging to II–IV semiconductor materials exhibits many favourable properties, such as wide bandgap (~ 3.3 eV), high exciton binding energy (~ 60 meV) and high chemical stability. Moreover, it is abundant in nature, non-toxic and environmentally friendly, while its growth requires low cost [1–5]. Over the last decades, zinc oxide has been extensively investigated with the purpose of its utilization in various industries and technologies. These are spintronics, light emitting diodes, laser diodes, sensors, varistors, heat mirrors, gamma-radiation sensing layers, pressure sensors, surface acoustic-wave devices, and transparent electrodes for solar cells and displays [6–16].

A number of physical and chemical methods have been used to fabricate high-quality thin ZnO films: molecular beam epitaxy [17], direct-current and radio-frequency magnetron sputtering [18], metal-organic chemical vapour deposition [19], dip coating [20], spin coating [21], electro-deposition [22], spray pyrolysis [23], and pulsed laser deposition [5]. Notice also that doping of ZnO with transition-metal elements has offered a feasible means for fine-tuning of the bandgap and, eventually, such applications as UV detectors and light emitters [24]. Chromium is a typical transition-metal element with especially abundant electron-shell structure and, moreover, the ionic radius of Cr^{3+} is close to that of Zn^{2+}. This means that Cr^{3+} can easily substitute Zn^{2+} in ZnO lattice [25]. It is worthwhile that doping of non-magnetic semiconductors with the transition metals (e.g., with Co, Ti, V, Cr, Mn, Fe, Ni and Cu) produces so-called diluted magnetic semiconductors, which are regarded as important materials for spintronic and photonic devices. Cr-doped thin films of ZnO have also attracted a close attention of researchers because the material reveals good chemical stability with respect to etching and a ferromagnetism phenomenon at the room temperature [25–27].

In particular, ZnCoO films which can be produced in an inexpensive manner exhibit high electron mobility, good optical transparency and high electrical conductivity [28]. The studies on

the ternary ZnCoO semiconductors have been greatly stimulated by a high Curie temperature of their ferromagnetic transition. It has been calculated for the bulk material and found to be around 300 K [29].

ZnMnO has a great potential to become a multifunctional material with interesting magnetic, semiconducting and optical properties [30]. So, ZnMnO is regarded to be promising for different spintronic applications since it manifests a room-temperature ferromagnetism [31]. Unfortunately, there is still an insufficient number of works dealing with the structure, morphology and optical properties of ZnCrO, ZnMnO and ZnCoO layers (see Refs. [30–38]). It has been demonstrated earlier that the optical transmission spectra and the optical bandgap energy of the pure ZnO layers depend strongly on both growth conditions and post-growth treatment [5, 18, 20, 23]. In the present work we study the optical properties of thin ZnCrO, ZnMnO and ZnCoO films, which are obtained by a pulsed laser deposition technique on sapphire substrates, before and after annealing.

2. Experimental

Thin ZnCrO films on sapphire substrates were obtained at the Drohobych State University (Ukraine), using a pulsed laser deposition method in the vacuum 10^{-5} Pa. For this aim a KWO_4 laser was employed, with the repetition rate 20 pulse/min and the pulse energy 0.2 J. The deposition time was equal to 30 min and the pulse duration to 20 ns. Targets with the compositions $Zn_{0.96}Cr_{0.04}O$, $Zn_{0.80}Cr_{0.20}O$, $Zn_{0.96}Mn_{0.04}O$, $Zn_{0.96}Co_{0.04}O$ were used. The ZnMnO films on sapphire substrates prepared from the $Zn_{0.80}Mn_{0.20}O$ target were obtained by the same pulsed laser deposition technique at the University of Rzeszow (Poland), using the second harmonic of YAG:Nd laser with the repetition rate 50 pulse/min. Here the vacuum was equal to $3.37 \cdot 10^{-4}$ Pa and the substrate temperatures were either 20°C or 250°C.

The optical transmission spectra of the thin films under test were recorded with a CARY 5000 spectrophotometer. Additionally, the samples were annealed during 5 min in the air (a NABERTHERM LH04 furnace) at the temperature 400°C. The transmission spectra were measured after annealing or, more exactly, after the samples had been cooled.

3. Results and discussion

The optical transmission spectra for the as-grown ZnCrO, ZnMnO and ZnCoO layers and for the sapphire substrate itself are shown in Fig 1. The spectra for the ZnCrO samples depend strongly on the target composition. For instance, the optical transmission of the sample obtained with 20% of Cr in the target (sample No 1, according to our notation) is significantly higher than that obtained in case of the target with the 4% of Cr content (sample No 2). This effect is different from that reported in Ref. [32] where the changes in the Cr^{3+} content in the region 1–8% influence only slightly the transmission of ZnCrO layers, and that described in Ref. [30] where the transmission of samples decreases with increasing chromium content (3–6% Cr).

The ZnMnO samples have been deposited from the target with 4% (sample No 3) or 20% Mn content at the substrate temperatures 20°C (sample No 4) and 250°C (sample No 5). The optical transmission of the sample No 5 in the spectral region 200– 850 nm is higher than that recorded for the other samples. Finally, the sample ZnCoO (sample No 6) has been deposited from the target with 4% of Co content. The transmission for this sample does not exceed 5% (not shown in Fig. 1). We are to note that the substrate temperature also notably affects the optical spectra for $Zn_{0.80}Mn_{0.20}O$ layers. As an example, the layer obtained at the substrate temperature 250°C has higher optical transparency in the visible region than that obtained at 30°C.

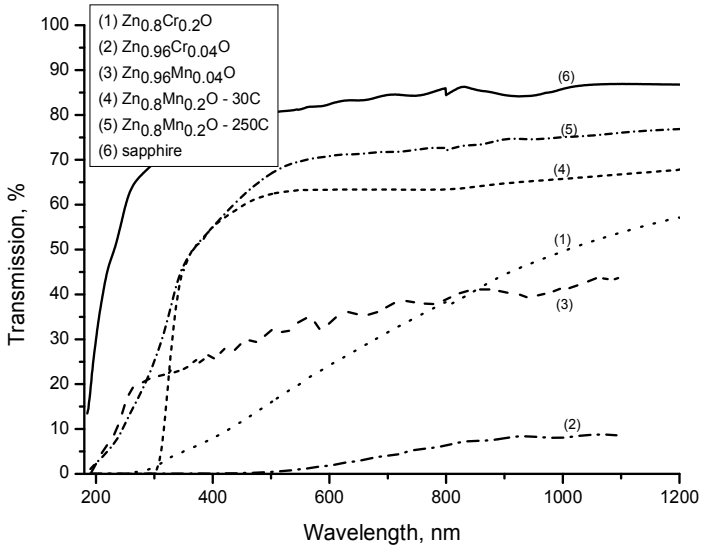

Fig. 1. Optical transmission spectra detected for as-grown $Zn_{0.80}Cr_{0.20}O$ (1), $Zn_{0.96}Cr_{0.04}O$ (2), $Zn_{0.96}Mn_{0.04}O$ (3), $Zn_{0.80}Mn_{0.20}O$ at 20°C (4), $Zn_{0.80}Mn_{0.20}O$ at 250°C (5), and sapphire (6).

The absorption edge of our samples can be approximated using a well-known Tauc relation [39] (see Fig. 2):

$$\alpha h\upsilon = B(h\upsilon - E_g)^m, \tag{1}$$

where E_g is the optical bandgap, h the Planck constant, υ the frequency of incident photons, B a constant, and m the index which can acquire different values. In particular, we have m = 2, 3, 1/2 and 1/3 respectively for indirect allowed, indirect forbidden, direct allowed and direct forbidden optical transitions. In our case, the approximation with m = 1/2 is satisfactory for all of the samples. This corresponds to the direct allowed transitions, which have been earlier observed for the pure ZnO layers [20].

In case of the direct transitions, the optical bandgap for the films can be determined using a transformed version of Eq. (1),

$$(\alpha h\nu)^2 = A(h\nu - E_g)\,. \tag{2}$$

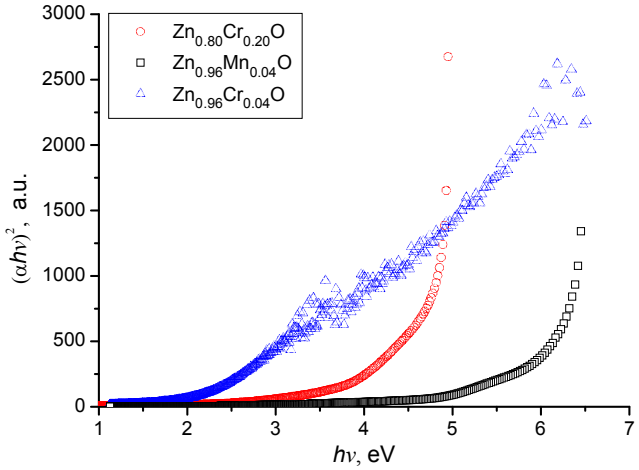

Fig. 2. Dependences of optical absorption on the photon energy in Tauc coordinates, as obtained for some of our samples.

Fig. 2 shows an example plot of the $(\alpha hv)^2$ parameter versus the photon energy. It enables one to obtain the energy gap with a sharp edge absorption, using a simple linear approximation approach. The E_g values calculated in this manner for the as-grown layers are gathered in Table 1.

Table 1. Bandgap values calculated for the samples corresponding to as-grown and annealed states.

Sample	Bandgap E_g, eV					
	Sample No 1	Sample No 2	Sample No 3	Sample No 4	Sample No 5	Sample No 6
Before annealing	4.82	2.40	5.96	2.95	3.94	1.96
At 400°C	3.43	4.00	5.91	2.97	3.97	3.46

The E_g value depends essentially on the samples, ranging in a wide interval from 1.96 to 5.96 eV. The E_g parameters known from the literature for ZnO are also located in a wide enough region, 3.24–5.87 eV [40, 41]. The differences in E_g can be partially due to different degrees of crystallinity typical for different samples. In particular, the authors of Ref. [20] have revealed that a blue shift of the absorption edge can be due to poor crystallinity of thin ZnO films. Due to a lack of long-range translational periodicity, the inter-atomic distances in the relevant amorphous structure would be longer and more disordered, if compared to that peculiar for the crystalline structure. As a consequence, the absorption of photons is dominated by the amorphous ZnO component and, hence, the absorption edge turns out to be blue-shifted [20]. We note also that the bandgap of ZnO depends on the film thickness [20]. Small transmittances observed for the samples No 2 and No 6 and their low E_g values can be due to the presence of Zn particles in the layers, together with ZnO. These phenomena will be explained in a more detail in our forthcoming works.

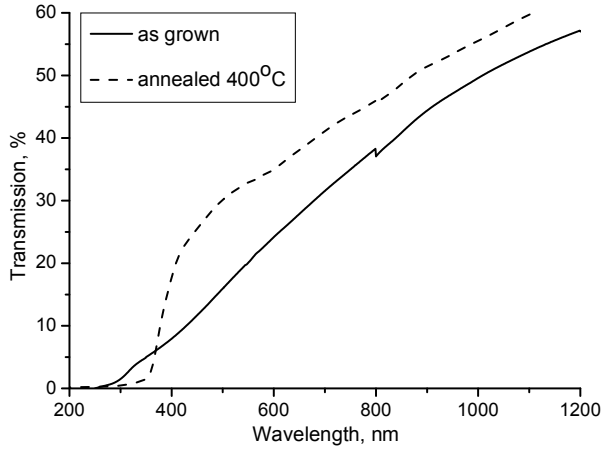

Fig. 3. Transmission spectra for the sample No 1 ($Zn_{0.8}Cr_{0.2}O$) detected before and after its annealing.

Annealing of the sample No 1 in the air at the temperature 400°C decreases the optical transmission below 370 nm and increases the transmittance above 370 nm (see Fig. 3). The optical energy gap decreases strongly after the sample is annealed at 400°C (see Table 1). Annealing of the sample No 2 at the temperature of 400°C leads to significant transmission increase if compared to the sample No 1 (see Fig. 4). Here the optical bandgap E_g increases after annealing by about 1.7 times (see Table 1). This effect is opposite to that found for the sample No 1 (see Table 1). In case of the sample No 6, the changes in the transmission observed after annealing have the same character as those typical for the sample No 2.

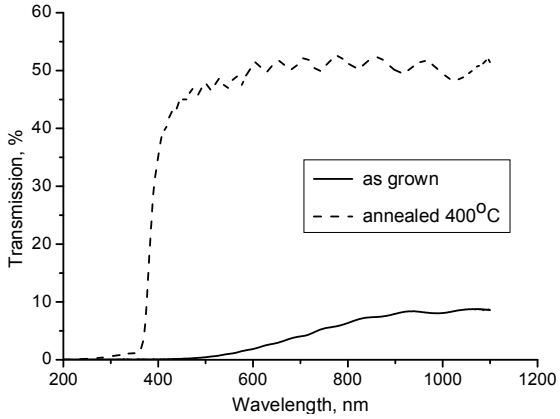

Fig. 4. Transmission spectra for the sample No 2 ($Zn_{0.96}Cr_{0.04}O$) detected before and after its annealing.

After annealing of the sample No 3 in the air at the temperature 200°C, a strong increase in the transmission is observed (see Fig. 5). Annealing at 400°C leads to transmission decrease (Fig. 5) but the transmission at the wavelengths shorter than 435 nm is still greater than that detected before annealing. Some E_g changes are also observed, although they are smaller than those seen for the other samples (see Table 1). Annealing of the samples No 4 and No 5 increases slightly their optical transmission (see Fig. 6). However, for the sample No 5 it is practically immeasurable.

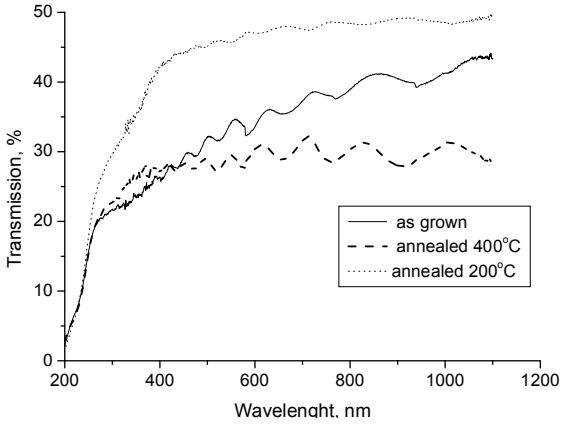

Fig. 5. Transmission spectra for the sample No 3 ($Zn_{0.96}Mn_{0.04}O$) detected before and after its annealing.

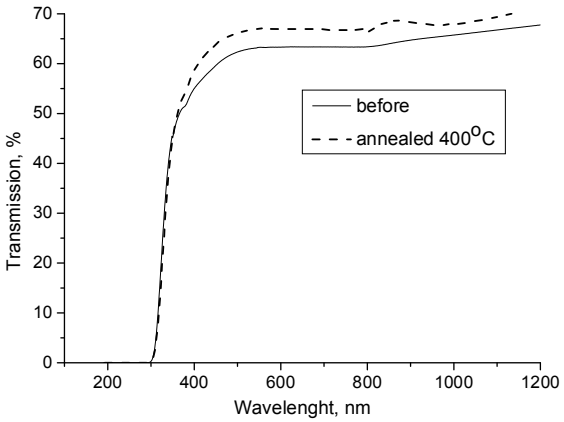

Fig. 6. Transmission spectra for the sample No 4 ($Zn_{0.80}Mn_{0.20}O$) detected before and after its annealing.

A small optical transmittance of the ZnCoO sample No 2 can be due to Zn particles which are present in the layers, together with ZnO. The post-growth annealing can lead to oxidation of Zn and producing of ZnO particles. This mechanism can also explain significant E_g changes occurring after heating. The work [42] dealing with the zinc nitride films has demonstrated that oxidized films reveal higher bandgap and transmittance in the short-wavelength spectral region, if compared with the appropriate parameters typical for the non-oxidized films. The reason is formation of $ZnO/Zn(OH)_2$ phase. We notice also that a fine-polycrystalline structure has been found for the sample No 6 before it is heated. After annealing, the coarse-grained polycrystalline structure has been detected with the TEM method. Such changes can partially affect the increase in the transmission detected after annealing [23].

4. Conclusion

Summarizing, we have found in the present work that the target composition and the kind of doping affect strongly the optical transmission spectra of the ZnTMO (TM = Cr, Co and Mn) layers and their optical bandgap energy. The $Zn_{0.96}Cr_{0.04}O$ and $Zn_{0.96}Co_{0.04}O$ layers are poorly permeable, but annealing at the temperature 400°C improves significantly their transmission. The post-growth annealing in the air leads to increasing optical transmission for all of our samples, except for the sample No 3 heated up to 400°C. We have also shown that the E_g value depends on the target composition and the character of doping. Moreover, it changes after the samples are annealed.

References

1. Lee JH, Ko KH, Park BO, 2003. Electrical and optical properties of ZnO transparent conducting films by the sol–gel method. Journ.Cryst.Growth, **247**: 119–125.
2. Virt IS, Hadzaman IV, Bilyk IS, Rudyi IO, Kurilo IV, Frugynskyi MS, Potera P, 2010. Properties of ZnO and ZnMnO thin films obtained by pulsed laser ablation. Acta Physica Polonica A, **117**: 34–37.
3. Konenkamp R, Boedecker K, Lux-Steiner M, Poschenrieder CM, Zenia F, Levy-Clement C, Wagner S, 2000. Thin film semiconductor deposition on free-standing ZnO columns. Appl. Phys. Lett. **77**: 2575–2576.
4. Singh S, Kaur H, Pathak D, Bedi R.K, 2011. Zinc oxide nanostructures as transparent window layer for photovoltaic application. Dig. Journ. Nanomat. Biostr. **6**: 689–698.
5. Wisz G, Virt I, Sagan P, Potera P, Yavorskyi R, 2017. Structural, optical and electrical properties of zinc oxide layers produced by pulsed laser deposition method. Nanoscale Res. Lett., **12**: 253.
6. Phan TL, Sun Y.K, Vincent R, Cherns D, Nghia NX, Yu SC, 2008. Optical properties of Mn-doped ZnO nanowires. Journ. Korean Phys. Soc., **52**: 1633–1636.
7. Ryu YR, Lee TS, Lubguban J A, White HW, Park YS, Youn CJ, 2005. ZnO devices: Photodiodes and pp-type field-effect transistors. Appl. Phys. Lett. **87**: 153504.
8. Ngan PH, Tien NQ, Dat DT, Nho PV, Nghia NX, Yu SC, 2008. Preparation of the transparent conductive ZnO nanomaterial by means of pulsed spray pyrolysis. Journ. Korean Phys. Soc. **52**: 1594–1597.
9. Özgür Ü, Alivov YaI, Liu C, Teke A, Reshchikov MA, Doğan S, Avrutin V, Cho S-J, Morkoç H, 2005. A comprehensive review of ZnO materials and devices. Journ. Appl. Phys. **98**: 041301.
10. Khranovskyy V, Eriksson J, Lloyd-Spetznita A, Yakimova R, Hultman L, 2009.Effect of

oxygen exposure on the electrical conductivity and gas sensitivity of nanostructured ZnO films. Thin Sol.Films **517**: 2073–2078.
11. Lorite I, Rubio-Marcos F, Romero J.J, Fernández J.F, 2009. In situ formation of Mn-doped ZnO aligned structures by rapid heating method. Mat.Lett. **63**: 212–214.
12. Girija K.G, Somasundaram K, Topkar A, Vatsa R.K, 2016. Highly selective H_2S gas sensor based on Cu-doped ZnO nanocrystalline films deposited by RF magnetron sputtering of powder target. Journ. Alloys Comp. **684**: 15–20.
13. Ya KX, Yin H, De TM, Jing TM, 1998. Analysis of ZnO varistors prepared from nanosize ZnO precursors. Mat. Res. Bull. **33**: 1703–1708.
14. Chopra KL, Major S, and Pandya DK, 1983. Transparent conductors – A status review. Thin Sol. Films **102**: 1–46.
15. Arshak K, Corcoran J, Korostynska O, 2005. Gamma radiation sensing properties of TiO2, ZnO, CuO and CdO thick film pn-junctions. Sens. Actuat. A **123–124**: 194–198.
16. Arora A, Dwivedi VK, George PJ, Sreenivas K, Gupta V, 2008. Zinc oxide thin film-based MEMS acoustic sensor with tunnel for pressure compensation. Sens. Actuat. A, **141**: 256–261.
17. Look DC, Reynolds DC, Litton CW, Jones RL, Eason DB, Cantwell G, 2002. Characterization of homoepitaxial p-type ZnO grown by molecular beam epitaxy. Appl. Phys. Lett. **81**: 1830.
18. Cho S, 2009. Effects of growth temperature on the properties of ZnO thin films grown by radio-frequency magnetron sputtering. Trans. Elect. Electron.Mat. **10**: 185–188.
19. Tan ST, Chen BJ, Sun XW, Fan WJ, Kwok HS, Zhang XH, Chua SJ, 2005. Blue shift of optical band gap in ZnO thin films grown by metal-organic chemical-vapor deposition. Journ. Appl. Phys. **98**: 013505.
20. Kayani ZN, Qbal M, Riaz S, Zia R, Naseem S, 2015. Fabrication and properties of zinc oxide thin film prepared by sol-gel dip coating method. Mat. Sci.-Pol. **33**: 515-520.
21. Srinivasan G, Gopalakrishnan N, Yu YS, Kesavamoorthy R, Kumar J, 2008.Influence of post-deposition annealing on the structural and optical properties of ZnO thin films prepared by sol–gel and spin-coating method. Superlatt.Microstr. **43**: 112–118.
22. Dalchiele EA, Giorgi P, Marotti R, Martín EF, Ayouci R, Leinen D, 2001. Electrodeposition of ZnO thin films on n-Si(1 0 0). Sol.Ener.Mat. Sol.Cells **70**: 245–254.
23. Nadarajah K, Chee CY, Tan CY, 2013. Influence of annealing on properties of spray deposited ZnO thin films. Journ.Nanomat. (Article ID 146382).
24. Senthilkumaar S, Rajendran K, Banerjee S, 2008. Influence of Mn doping on the microstructure and optical property of ZnO. Mat.Sci.Semicond.Proc. **11**: 6–12.
25. Liua Y, Yang J, 2009. Effects of Cr-doping on the optical and magnetic properties in ZnO nanoparticles prepared by sol–gel method. Journ.Alloys Comp. **486**: 835–838.
26. Olvera MD, Maldonado A, Asomoza R, Lira MM, 2000. Chemical stability of doped ZnO thin films. Journ. Mat.Sci.: Mat. Electron. **11**: 1–5.
27. Sato K, Yoshida HK, 2001. Stabilization of ferromagnetic states by electron doping in Fe-, Co- or Ni-Doped ZnO. Jap. Journ.Appl.Phys. **40**: L334–L336.
28. Benramache S, Benhaoua B, Chabane F, 2012. Effect of substrate temperature on the stability of transparent conducting cobalt doped ZnO thin films. Journ.Semicond. **33**: 093001–1.
29. Dietl T, Ohno H, Matsukura F, 2001.Hole-mediated ferromagnetism in tetrahedrally coordinated semiconductors. Phys.Rev.B **63**: 195205.
30. Mandal S.K, Nath T.K, 2006. Microstructural, magnetic and optical properties of ZnO:Mn ($0.01 \leq x \leq 0.25$) epitaxial diluted magnetic semiconducting films. Thin Sol.Films **515**: 2535–2541.

31. Singhal RK, Dhawan M, Kumar S, Dolia SN, Xing YT, Saitovitch E, 2009. Room temperature ferromagnetism in Mn doped dilute ZnO semiconductor; an electronic structure stud. Physica B **404**: 3275–3280.
32. Iqbal A, Ahmood A, Khan TM, Ahmed E, 2013. Structural and optical properties of Cr doped ZnO crystalline thin films deposited by reactive electron beam evaporation technique. Prog.Nat.Sci.: Mat.Intern. **23**: 64–69.
33. Ramani RV, Ramani BM, Saparia AD, Savaliya C, Rathod KN, Markna JH, 2018. Cr–ZnO nanostructured thin film coating on borosilicate glass by cost effective sol–gel dip coating method. Ain Shams Engin. Journ. **9**: 777–782.
34. Maldonado A, Mall´En-Hern´Andez SA, Vega-P´Erez J, Olvera M L, Tirado-Guerra S, 2009. Chromium doped zinc oxide thin films deposited by chemical spray used in photo-catalysis and gas sensing. Rev.Mexic.Fis. **S55**: 90–94.
35. Iqbal T, Ghazal S, Atiq S, Khalid NR, Majid A, Afsheen S, Niaz NA, 2016. Influence of manganese on structural, dielectric and magnetic properties of ZnO nanoparticles. Digest Journ. Nanomat. Biostr. **11**: 899 – 908.
36. Mondal S, Bhattacharyya SR , Mitra P, 2013.Preparation of manganese-doped ZnO thin films and their characterization. Bull.Mat.Sci. **36**: 223–229.
37. Cao P, Bai Y, 2013.Structural and optical properties of ZnCoO thin film prepared by electrodeposition. Advan.Mat.Res. **781–784**: 323–326.
38. Vuichyk MV, Tsybrii ZF, Lavoryk SR, Svezhentsova KV, Virt IS, Chizhov A, 2014. Morphologic and optical characterization of ZnO:Co thin films grown by PLD. Semicond.Phys.Quant.Electron. & Optoelectron. **17**: 80-84.
39. Viezbicke BD, Patel S, Davis BE, Birnie DP, 2015. Evaluation of the Tauc method for optical absorption edge determination: ZnO thin films as a model system. Phys.Stat.Sol. B, **252**: 1700–1710.
40. Nithya N, Radhakrishnan S, 2012. Effect of thickness on the properties ZnO thin films. Advan.Appl.Sci.Res. **3**: 4041–4047.
41. Khan ZR, Khan MS, Zulfequar M, Khan MoS, 2011. Optical and structural properties of ZnO thin films fabricated by sol-gel method. Mat.Sci.Appl. **2**: 340–345
42. Trapalis A, Heffernan J, Farrer I, Sharman J, Kean A, 2016. Structural, electrical, and optical characterization of as grown and oxidized zinc nitride thin films. Journ.Appl. Phys. **120**: 205102.

Анотація. *Вивчено оптичні властивості шарів цинково-хромового (ZnCrO), цинково-марганцевого (ZnMnO) і цинково-кобальтового (ZnCoO) оксидів, вирощених на сапфірових підкладках, використовуючи техніку імпульсну лазерного висадження. Проаналізовано вплив вихідного складу та післяростового відпалу на оптичне пропускання плівок і їхню ширину забороненої зони.*

Potera P., Virt I., Cieniek B. and Wisz G. 2019. Optical properties of ZnO:TM (TM = Cr, Mn and Co) layers obtained by pulsed laser deposition technique. Ukr.J.Phys.Opt. **20**: 143 – 150.
doi: 10.3116/16091833/20/4/143/2019